Effect of Standoff Distance on the Partitioning of Surface Heat Flux during Subcooled Jet Impingement Boiling

S. Abishek †, R. Narayanaswamy †, V. Narayanan ‡

† Department of Mechanical Engineering, Curtin University, Perth, WA, 6102, Australia
‡ School of Mechanical, Industrial and Manufacturing Engineering, Oregon State University, Corvallis, OR, 97331, USA

Abstract

Heat transfer involving boiling of impinging jets are used for cooling components that dissipate very large heat fluxes, typically over 100 W/cm^2 concentrated at discrete locations. Several industrial applications requiring cooling of discretely heated components such as in power electronics, synchrotron x-ray, fusion, and semiconductor laser systems have found beneficial use of boiling impinging jets, particularly due to the large heat transfer coefficients obtained in the stagnation region. The present paper aims to investigate the effect of standoff distance on the partitioning of the surface heat flux during subcooled and confined submerged jet impingement boiling, for different heater sizes. The RPI wall-boiling model is employed for the partitioning of surface heat flux into liquid phase convective, quenching and evaporative heat fluxes, and solved in conjunction with the governing equations for flow and heat transfer. It is found that the standoff distance influences the characteristics of boiling only in the partial nucleate boiling regime. Besides, the influence was only on the liquid phase convective component of the total heat flux, while the quenching and evaporative components remained unaffected. The total heat flux in the partial nucleate boiling regime was consistently larger for smaller standoff distances, irrespective of the heater size. The change in the surface averaged liquid phase convective heat flux with change in standoff distance was also found to be larger for relatively smaller heater sizes in the partial nucleate boiling regime.

Keywords: nucleate boiling; jet impingement; RPI model; standoff distance; numerical

Nomenclature

B	width of slot-nozzle (mm)
q_C	liquid phase convective heat flux (W/m^2)
q_E	evaporation heat flux (W/m^2)
q_Q	quenching heat flux (W/m^2)
q_T	total surface heat flux (W/m^2)
Re	Reynolds number based on hydraulic diameter
ΔT_{sat}	degree of saturation (^{o}C)
ΔT_{sub}	degree of subcooling (^{o}C)
W	width of heater (mm)
w	dimensionless width of heater
Z	standoff distance (mm)
z	dimensionless standoff distance

Symbols

ρ	density (kg/m^3)
μ	dynamic viscosity (Pa s)

Subscripts

expt	experiment
pred	prediction

Introduction

Impinging jets are very effective in cooling very large heat fluxes concentrated at discrete locations. Several industrial applications including cooling/ quenching of metals during metal processing, cooling of power electronic components, synchrotron x-ray systems, fusion, and semiconductor laser systems have found beneficial use of boiling impinging jets due to the high heat transfer rated obtained at the impinging stagnation region [1-3].

In the last few decades, several experimental investigations have been carried out to investigate the effects of the controlling parameters on the boiling of submerged impinging liquid jets. Wolf et al. [4] presented a detailed review of the literature on free surface, plunging and submerged (both confined and unconfined environments) jet impingement boiling, for both subcooled and saturated conditions. It is seen that among several parameters that control the characteristics of jet impingement boiling, the standoff distance is particularly interesting as there are specific ranges for combinations of other controlling parameters in which the characteristics of boiling are influenced. Mudawar & Wadsworth [5] carried out extensive experiments to understand the relationship between the critical heat flux and the governing parameters such as jet velocities, heater sizes, heater spacings and inlet subcooling, for an impinging slot jet of FC-72. They showed that there existed two distinct regimes of CHF depending on the velocities and standoff distance, and that it could result in an otherwise reduction of CHF with increase in velocity for relatively smaller standoff distances, due to a stream-wise reduction in liquid subcooling in the domain. More recently, Shin et al. [6] showed that the effect of standoff distance on fully developed boiling of an impinging jet of PF-5060 was larger for lower standoff distances. It was also shown that the critical heat flux decreased with increase in the standoff distance to nozzle size ratio of about 1-2 and subsequently increased with any further increase in the ratio, for jet Reynolds numbers in the range 2000-5500. Aihara et al. [7] also showed that the characteristics of boiling of an impinging submerged jet of nitrogen resulted in an attendant decrease in the wall superheat with decrease in nozzle to heater spacing, for a concave radially confined geometry. However, a few studies [8,9] also showed that the influence of the standoff distance on the characteristics of jet impingement boiling is very minimal.

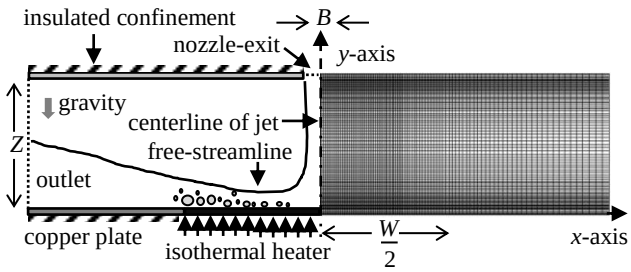

Figure 1: Physical geometry and computational domain

A review of the literature on jet impingement boiling suggests that the almost all the investigations on the subject have been experimental, with very few computational analyses. The state of the art on numerical analysis of jet impingement boiling has been detailed in Abishek et al. [10], and hence omitted here for brevity. This present paper aims to investigate the effect standoff distance using computational simulations of subcooled confined submerged jet impingement boiling, on the partitioning

of the surface heat flux, and hence, the boiling curves, for different values of the heater sizes and a fixed Reynolds number.

Problem Description and Computational Domain

A schematic of the problem analyzed is shown in Fig. 1, wherein, the computational domain and the mesh are indicated on the right side of the centerline of jet. A fully developed turbulent water-jet at a temperature of 75°C (ΔT_{sub}=25 °C) and average velocity of 0.438 m/s (hydraulic diameter based Re = 5400) exits a slot of width B = 2 mm, into a quiescent medium of water at the same temperature and at atmospheric pressure. The fully developed velocity profile at the outlet of the nozzle was determined from a simulation of flow in a two dimensional duct of length 50×slot-width. The polished impingement surface (copper plate of length 30 mm and thickness of 200 μm) is heated from below upto a length $W/2$ = 3 mm or 10 mm ($w = W/B$ = 3 or 10) on either sides of the centerline of jet, while the rest of the plate is thermally insulated from below. The flow passage is sandwiched between the copper plate and externally insulated polycarbonate confinement blocks placed at the plane of the nozzle-exit, such that the standoff distance is Z = 4 mm, 12 mm or 16 mm ($z = Z/B$ = 2, 6 & 8). Symmetry about the centerline of the jet is exploited to carryout numerical simulations on one-half of the domain alone. The outlet of the domain is assumed to be at atmospheric pressure, free of vapor and at the same liquid temperature as that at the nozzle-outlet. All other parts of the heater and the sides of the polycarbonate confinement are assumed to be thermally insulated. It is to be noted that a conjugate heat transfer analysis is considered (conduction in the copper plate is included) to ensure a realistic representation of the physical problem. A spatially varying structured non-uniform rectangular mesh is used for the simulations, where the mesh is fine near the walls and the centerline of jet, and relatively larger near the outlet of the domain as shown on the right hand side of the illustration in Fig. 1. It was also ensured that the wall $y+ \leq 4$ on the impingement surface, as the viscous sublayer was modeled in the simulation (without using standard turbulent wall functions) for increased prediction accuracy. All the simulations carried out for the present research (excluding validation) were with the assumption of constant fluid properties.

Mathematical Modeling

The governing equations of mass, momentum, energy, turbulence along with the closures for wall heat-flux partitioning are solved using the finite volume based solver ANSYS-FLUENT. The *Quadratic Upstream Interpolation for Convective Kinematics* (QUICK) numerical scheme is employed for the governing equations of continuity, momentum and energy, while a modified *High Resolution Interface Capturing* (HRIC) scheme is employed for volume fraction. The flow and heat transfer are predicted by considering the liquid and vapor phases to be an Euler-Euler interpenetrating continua. The equations of continuity, momentum and energy are solved for each phase, while turbulence is solved by considering the medium to be a mixture. The *Re-Normalization Group* (RNG) k-ε mixture model [11-14] with enhanced wall treatment is adopted for modeling turbulence. The surface heat flux for partial and fully developed nucleate boiling is modeled as the sum of liquid phase convection, quenching (typically modeled using transient conduction) and evaporation, and solved with the closures, in accordance with the *Rensselaer-Polytechnic Institute* (RPI) wall-boiling model [15]. The interfacial momentum transfer is modelled using appropriate correlations for the drag, lift and turbulent dispersion forces, and interphase heat transfer is modelled using the Ranz-Marshall correlation [16]. For brevity, only the partitioning of heat flux using the RPI wall-boiling model is included hereunder; while the detailed set of governing equations and closures can be found from Abishek et al. [10].

Wall Heat-Flux Partitioning

The total heat transfer rate from the solid heater surface to the fluid undergoing nucleate boiling is partitioned into three components *viz*., heat transfer due to the liquid phase convection (q_C), quenching (q_Q), and evaporation (q_E). Hence the net heat flux (q_T) at the solid-fluid interface is

$$q_T = q_C + q_Q + q_E \tag{1}$$

The three components of the heat flux in the RPI wall-boiling model are evaluated as follows.

Liquid phase convective heat flux: At any instant of time during nucleate boiling, the surface over which boiling is expected to occur is divided into two areas: A_b, covered by the vapor bubbles; and (1-A_b), covered by the liquid. Hence, the convective heat flux is defined as

$$q_C = h_C\,(1-A_b)\,(T_w - T_l) \tag{2}$$

where, T_w and T_l are the local wall and liquid phase temperature respectively, and h_C is the liquid phase turbulent convective heat transfer coefficient defined by Egorov & Menter [17] using the near wall velocity field. This form of the heat transfer coefficient is practically more suitable for problems of the type in the present research, as compared to Kurul & Podowski's [18] Stanton number based correlation which is highly mesh dependant. The effective area occupied by the bubbles (A_b) is as [15]

$$A_b = \min\left[1,\ \left(\frac{\pi}{4}\xi N_w\, d_{bw}^2\right)\right] \tag{3}$$

where the area influence coefficient is defined according to De Valle & Kenning [19] as

$$\xi = 4.8\,e^{-0.0125 Ja_{sub}} \tag{4}$$

In the preceding equation, the Jacob number is defined as

$$Ja_{sub} = \rho_l c_{p_l} \Delta T_{sub} / \rho_v L \tag{5}$$

and the nucleation site density is defined according to Lemmert & Chawla [20] as

$$N_w = 200^{1.8}(T_w - T_{sat})^{1.8} \tag{6}$$

In the preceding equations, ρ_l, Cp_l, ΔT_{sub}, ρ_v , L and T_{sat} represent the density of liquid, specific heat of liquid, degree of inlet subcooling, vapor density, latent heat and saturation temperature, respectively. The bubble departure diameter (in meters) is defined according to Unal's correlation [21] as

$$d_{bw} = 2.42\times10^{-5}\, p^{0.709}\, \xi_1 / \sqrt{\xi_2\, \xi_3} \tag{7}$$

where p is the local pressure; and the parameters ξ_1 , ξ_2 and ξ_3 are defined as

$$\xi_1 = (T_w - T_{sat})/2\,L\,\rho_v \sqrt{k_s\, \rho_s\, C_s / \pi} \tag{8}$$

where k_s , ρ_s and C_s , are the thermal conductivity, density and specific heat of the impingement surface, respectively.

$$\xi_2 = \frac{0.5}{(1-\rho_v/\rho_l)} \times \max\left[(T_{sat} - T_l),\ \left(\frac{q_w}{6.5\times10^{-3}\rho_l\, c_{p_l} U_l}\right)\right] \tag{9}$$

and $$\xi_3 = \max\left[\left(U_l / 0.61\right)^{0.47}, 1\right] \tag{10}$$

where U_l is the liquid velocity in the cell adjacent to the wall.

Quenching heat flux: The quenching component of the total heat flux is modeled as the cyclic averaged transient energy transfer related to the liquid filling the vicinity of the wall, after bubble detachment [15]. Similar to the liquid phase convective heat flux, the quenching heat flux is given by,

$$q_Q = h_Q\, A_b\, (T_w - T_l) \tag{11}$$

where h_Q is the quenching heat transfer coefficient defined as

$$h_Q = 2 f \sqrt{\tau\, k_l \rho_l c_{p_l} / \pi} \tag{12}$$

where f is the bubble departure frequency [22], defined as

$$f = \sqrt{4g\left(\rho_l - \rho_v\right)/\left(3d_{bw}\rho_l\right)} \quad (13)$$

and $\tau = 0.8/f$ is the bubble waiting time (average time between any two consecutive bubble departure), defined according to Tolubinski & Kostanchuk [23] as about 80% of the bubble detachment period. The value of T_l used in Eq. (13) is evaluated at a fixed y^+ of 250 to avoid mesh dependant results, following [12,15].

Evaporation heat flux: The evaporative component of the total heat flux of the initially subcooled liquid is defined as

$$q_E = \left(\pi/6\right)d_{bw}^3 f N_w \rho_v L \quad (14)$$

where d_{bw}, f, N_w, ρ_l and L are bubble departure diameter, bubble departure frequency, nucleation site density, density of vapor and latent heat.

Validation

The results from the present numerical model were validated against three sets of experimental results pertaining to (i) confined slot jet impingement of PF-5060, (ii) unconfined round jet impingement of water, and (iii) pool boiling of water. The details of operating conditions, control variables and the geometries of the experimental configurations considered for validation are

	Mani et al. [24]	**Shin et al. [6]**	**Cardenas [27]**
Fluid	Deionized and degassed water	Dielectric fluid PF-5060	Deionized and degassed water
Schematic of problem	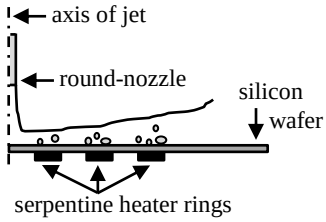	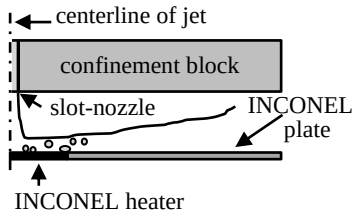	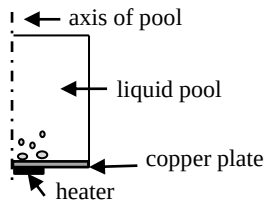
Operating pressure	101.325 kPa	101.325 kPa	101.325 kPa
Power input and heater type	442 W; discretized-uniform volumetric heat generation	6.4 to 32 W; uniform volumetric heat generation	10 to 120 W; uniform heating from below
Heater surface	380 µm thick; polished silicon	467 µm thick; polished INCONEL	200 µm thick; polished copper
Subcooling	≈ 20 °C	≈ 25 °C	≈ 20 °C
Reynolds number	2580 and 5161 based on nozzle diameter	1999 and 2751 based on slot width	Pool boiling

Table-1: Details of experimental studies considered for validation of the present numerical model

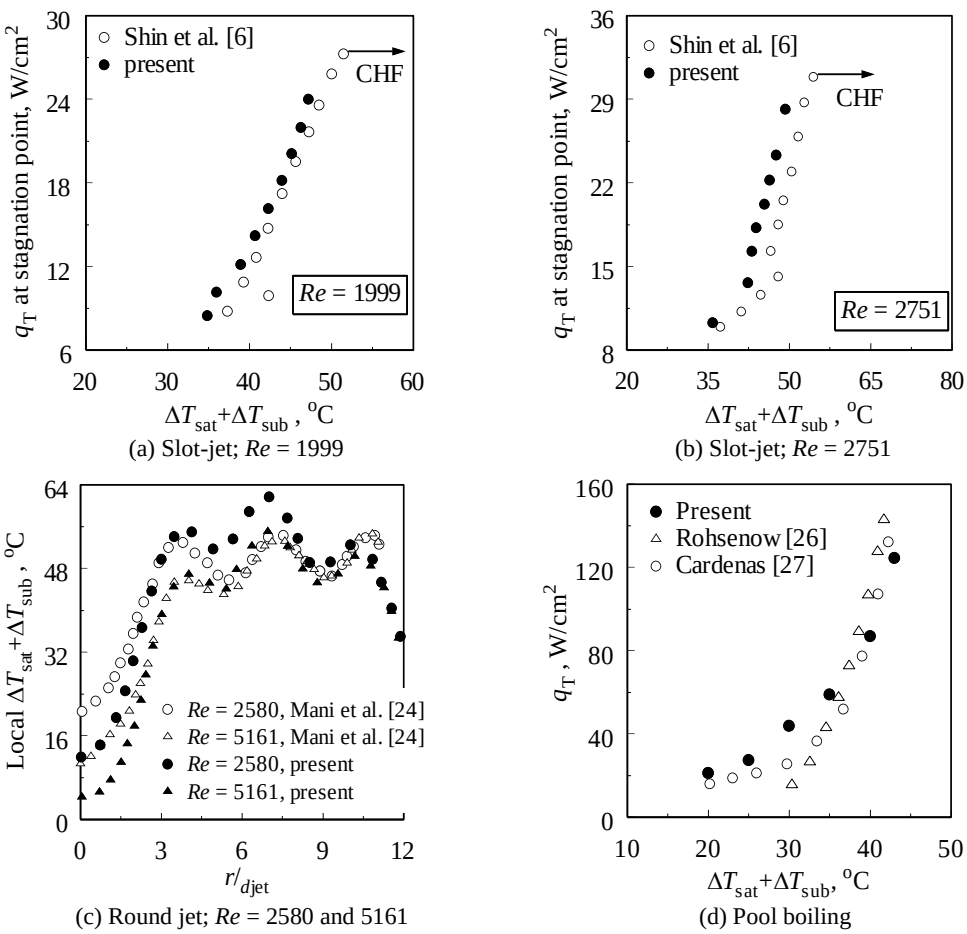

(a) Slot-jet; *Re* = 1999 (b) Slot-jet; *Re* = 2751

(c) Round jet; *Re* = 2580 and 5161 (d) Pool boiling

Figure 2: Validation of predicted local temperature and boiling curves against experimental data

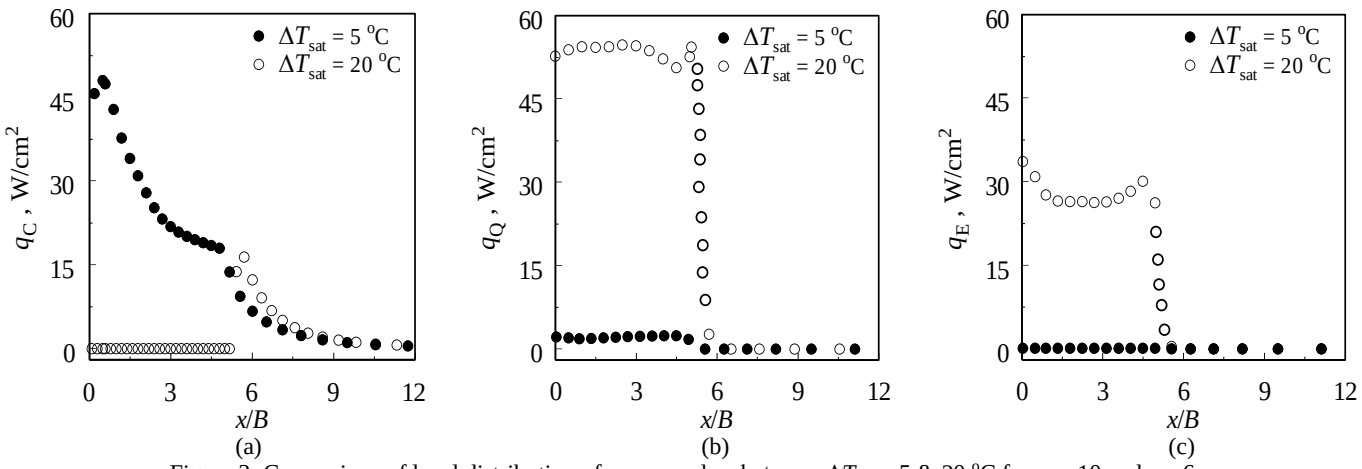

Figure 3: Comparison of local distribution of q_C, q_Q and q_E between ΔT_{sat} = 5 & 20 °C for w = 10 and z = 6

presented in Table-1.

Figure 2(a) and 2(b) show the local boiling curves at the stagnation point (for PF-5060 as working fluid) for jet Reynolds numbers of Re_w = 1999 & 2751, respectively. It is seen from the figures that the predicted local boiling curves are in good agreement with the experiments of Shin et al. [6]. The maximum absolute error in the predicted stagnation temperature in the operating range, defined as

$$Error = 1 - (\Delta T_{sat}+\Delta T_{sub})_{pred} / (\Delta T_{sat}+\Delta T_{sub})_{expt} \quad (15)$$

is found to be about 8% for Re = 2751 and less than about 2.5% for Re = 1999.

Figure 2(c) shows the surface temperature on the heater obtained from the present numerical simulations with water for two different jet Reynolds numbers (Re_d = 2580 & 5161) for a heater power of 442 W, superimposed on the experimentally obtained temperature distribution of Mani et al. [24]. It is seen from the figure that the predicted numerical results for the local temperature distribution on the silicon (impingement) surface are in good agreement with the experiments of Mani et al. [24]. The maximum absolute error in the local surface temperature is about ± 7 °C in the stagnation region and less than about ± 4 °C on the rest of the impingement-surface. It is also seen that the local peaks in the temperature distribution due to the radially discrete rings of the serpentine heater elements are captured accurately in the numerical simulations. Deviations of about 30% in the predicted surface temperature in the operating range have been reported in

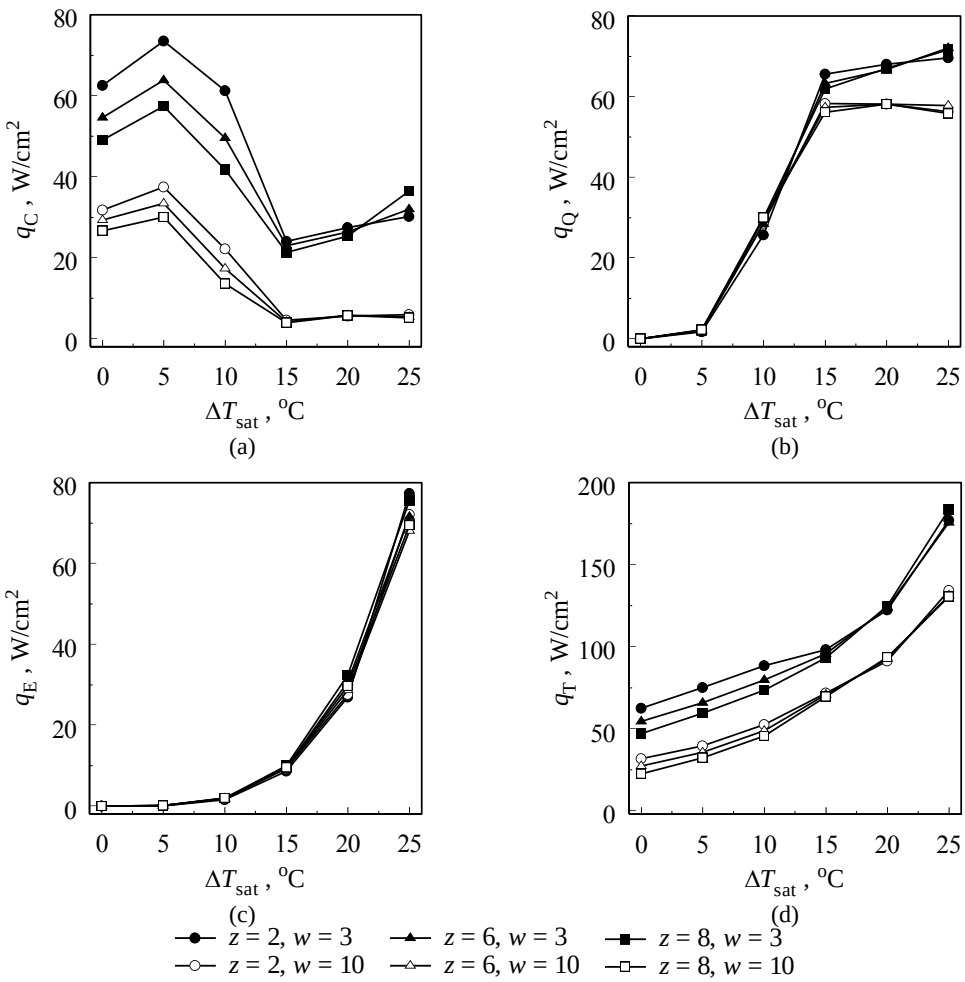

Figure 4: Comparison of boiling curves between three different standoff distances z = 2, 6 & 8 for two different heater sizes w = 3 & 10

the literature from similar numerical simulations [25].

Figure 2(d) shows the surface averaged boiling curve for pool boiling at atmospheric pressure on a round heater of radius 1 cm, superimposed with Rohsenow's correlation [26] and the experimental data of Cardenas [27]. It is once again seen that the predictions are in excellent agreement with the literature, thereby reinforcing the validity of the present simulation for modeling boiling heat transfer. The maximum absolute error in the predicted average surfaces temperature, against experimental data is about ± 11% in the operating range.

A grid independence test was carried out with five different mesh configurations with successively finer mesh in the near-wall regions, by observation of the change in wall $y+$ and the distribution of local surface heat flux. All further results presented herein were generated with the mesh shown on the right hand side of Fig. 1 with a $y+ \leq 4$ on the impingement surface, and the results are grid independent upto about 3%. As the problem considered involves a confined outflow, which partially consists of a wall-jet and partially reverse flow (circulation), any specified outlet pressure would not represent the real geometry, and would introduce numerical anomalies due to the superficially imposed pressure. Hence, the length of the domain beyond the heater was determined from the technique elucidated in Abishek et al. [10].

Effect of Standoff Distance

Figures 3(a-c) compare the distribution of local liquid phase convective, quenching and evaporative heat fluxes over the copper impingement surface between ΔT_{sat} = 5 & 20 ^{o}C for w = 10 and z = 6. It is seen from the figures that the liquid phase convective heat flux is the largest contributor to the total heat flux, with insignificant magnitudes of quenching and evaporative heat flux for ΔT_{sat} = 5 ^{o}C. On the contrary, the liquid phase convective heat flux is almost zero on the surface for ΔT_{sat} = 20 ^{o}C where the quenching and evaporative components contribute to the majority of the total heat flux. The reason for the convective component of the total heat flux not reducing to zero with at large surface superheats is because of the conduction in the impingement surface from the heated region to regions beyond the length of the heater, that results in single phase convective heat transfer. As shown in an earlier investigation [10], this comparison of the local heat flux distribution can be correlated to mean that the flow and heat transfer regime is partial nucleate boiling for ΔT_{sat} = 5 ^{o}C while it is fully developed nucleate boiling for ΔT_{sat} = 20 ^{o}C. Hence, it is evident that the transition from partial to fully developed nucleate boiling occurs in an interim value of ΔT_{sat}.

It is seen from Figs. 4(a-c) that beyond a threshold value, typically in the range 10 ^{o}C $\leq \Delta T_{sat} \leq$ 15 ^{o}C (or 35 ^{o}C $\leq \Delta T_{sat} + \Delta T_{sub} \leq$ 40 ^{o}C) there is a steep drop in the liquid phase convective heat flux, associated with a concomitant steep rise in the quenching and the evaporative heat fluxes. As shown by Abishek et al. [10] and Basu et al. [28,29], this trend can be correlated to the transition from partial nucleate boiling to fully developed nucleate boiling. It is also seen from Fig. 4(d) that the onset of fully developed nucleate boiling results in a subsequent rise in the total surface heat flux removed per unit change in heater temperature (note the increase in the slope of the curve).

It is seen from Figs. 4(a-d) that the surface averaged values of the liquid phase convective heat flux and the total heat flux are consistently larger for relatively smaller standoff distances while there is negligible change in the quenching and evaporative counterparts with change in standoff distance. As the total heat flux is modeled as the sum of the component heat fluxes in the current numerical model, the observed trend for q_T with change in standoff distance in the partial nucleate boiling regime can be perceived as a direct consequence of q_C. Recalling the discussion on Fig. 3(a-c) and Abishek et al. [10] that liquid phase convection is the dominant mode of heat transfer in the range of surface temperatures until fully developed nucleate boiling occurs, the average heat transfer is larger for relatively smaller standoff distances, as is the case for single phase jet impingement cooling. This is in-line with the literature on the investigation of single phase jet impingement heat transfer, such as in Martin [30], Lee & Lee [31] and Zuckerman & Lior [32]. Wolf et al. [33] showed that for surface temperatures beyond boiling incipience and within the partial nucleate boiling regime, boiling on the surface is limited to only a small number of vapor bubbles and the jet flow continues to strongly influence the heat transfer. The negligible difference in the boiling curves for the quenching and evaporative components of the total heat flux between z = 2, 6 & 8 in Figs. 4(b-c) implies the very abstemious relation between the standoff distance and the characteristics of fully developed nucleate boiling. It is also seen from the figures that the lithe effect of the standoff distance on quenching and evaporative heat fluxes is consistent irrespective of the heater size, for the range of parameters considered in the present research. Another observation from the comparison of Fig. 4(b) and Fig. 4(c) is that the effect of heater size is negligible in influencing the evaporative component of the surface heat flux, irrespective of the surface temperature, while its effect on the quenching heat flux is prominent only in the fully developed nucleate boiling regime. It is also seen that the variation of the liquid phase convective heat flux in the partial nucleate boiling regime with change in standoff distance is larger for w = 3 as compared to w = 10, implying a larger influence of the standoff distance for smaller heaters.

Conclusions

The effect of the standoff distance (nozzle-to-heater spacing) on the partitioning of surface heat flux as well as the total heat flux is studied for a confined submerged turbulent jet of de-ionized and degassed water impinging on a copper plate, at atmospheric pressure. Numerical modeling was based on the RPI wall heat flux partitioning. The present model was validated against three different cases *viz*. (i) unconfined axisymmetric round jet impingement of water on a non-uniformly heated silicon surface; (ii) confined slot impingement of PF-5060 on a uniformly heated INCONEL surface; and (iii) pool boiling of water on a uniformly heated copper surface. The range of parameters considered are Re = 5400, ΔT_{sub}=25 ^{o}C, w = 3 & 10, $2 \leq z \leq 8$. The salient conclusions of the research are as follows:

- The standoff distance influenced the characteristics of boiling only in the partial nucleate boiling regime, while the boiling curves in the fully developed nucleate boiling regime were unaffected, irrespective of the heater size
- In the partial nucleate boiling regime, only on the liquid phase convective component of the total heat flux was affected by standoff distance, while the quenching and evaporative components remained unaffected.
- The liquid phase convective heat flux, and hence, total heat flux in the partial nucleate boiling regime are consistently larger for smaller standoff distances, irrespective of the heater size.
- The change in the liquid phase convective heat flux with change in standoff distance in the partial nucleate boiling regime is larger for relatively smaller heaters.

Acknowledgements

S. Abishek was supported by Curtin International Postgraduate Research Scholarship to carry out the research; V. Narayanan would like to acknowledge the support of the National Science Foundation under award number 0748249.

References

[1] Narumanchi S.V.J., Troshko A., Bharathan D., Hassani V., Numerical Simulations of Nucleate Boiling in Impinging

Jets: Applications in power electronics cooling, *Int. J. Heat and Mass Transfer*, **51**, 2008, 1–12

[2] Leinhard J.H.V., Hounsary A.M., Liquid Impingement Cooling in Conjunction with Diamond Substrates for Extremely High Heat Flux Applications, *High Heat Flux Engineering II, Bellingham, WA: Society of Photo-Optical Instrumentation Engineers*, 1997, 29-43

[3] Liu X., Lienhard J.H.V., Extremely High Heat Fluxes Beneath Impinging Liquid Jets, *ASME J. Heat Transfer*, **115**, 1993, 472-476

[4] Wolf D.H., Incropera F.P., Viskanta R., Jet Impingement Boiling, *Adv. Heat Transfer*, **23**, 1993), 1-132

[5] Mudawar I., Wadsworth D.C., Critical Heat Flux from a Simulated Chip to a Confined Rectangular Impinging Jet of Dielectric Fluid, *Int. J. Heat and Mass Transfer*, **36**, 1991, 1465-1479

[6] Shin C. H., Kim K. M., Lim S. H., Cho H. H., Influences of Nozzle-Plate Spacing on Boiling Heat Transfer of Confined Planar Dielectric Liquid Impinging Jet, *Int. J. Heat and Mass Transfer*, **52**, 2009, 5293–5301

[7] Aihara T., Kim J. K., Suzuki K., Kasahara K., Boiling Heat Transfer of a Micro-impinging Jet of Liquid Nitrogen in a Very Slender Cryoprobe", *Int. J. Heat and Mass Transfer*, **36**, 1993, 169-175

[8] Monde M., Katto Y., Study of Burn-Out in a High Heat-Flux Boiling System with an Impinging Jet (Part-1, Behaviour of the Vapor-Liquid Flow), *Trans. JSME*, **43**, 1970, 3399-3407

[9] Kamata T., Kumagai S., Takeyama T., Boiling Heat Transfer to an Impinging Jet Sprouted into a Narrow Space (Part-1, Space with an Open End), *Heat Transfer-Japanese Res*. **17**, 1988, 71-80

[10] Abishek S., Narayanaswamy R., Narayanan V., Effect of Heater Size and Reynolds Number on the Partitioning of Surface Heat Flux in Subcooled Jet Impingement Boiling, *Int. J. Heat and Mass Transfer*, 2012, *accepted*

[11] Yakhot V., Orszag S.A., Thangam S., Gatski T.B., Speziale C.G., Development of Turbulence Models for Shear Flows by a Double Expansion Technique, *Phys. of Fluids-A*, **4**, 1992, 1510-1520

[12] Yakhot V., Orszag S.A., Renormalization-Group Analysis of Turbulence, *Phy. Review Letters*, **57**, 1986, 1722-1724

[13] Yakhot V., Orszag S.A., Renormalization-Group Analysis of Turbulence-I Basic Theory, *J.Scientific Computing*, **1,** 1986, 3-51

[14] Yakhot V., Smith L.M., The Renormalization-Group- The e{open}-Expansion and Derivation of Turbulence Models, *J. Scientific Computing*, **7**, 1992, 35-61

[15] ANSYS FLUENT Theory Guide, Release 13.0, November 2010, ANSYS Inc.

[16] Ranz W.E., Marshall Jr. W.R., Evaporation from Drops, Part-1 & Part-2, *Chem. Eng. Prog.*, **48**, 1952, 173-180

[17] Egorov Y., Menter F., Experimental Implementation of the RPI Wall Boiling Model in CFX-5.6, *Technical Report ANSYS/TR-04-10*, ANSYS Germany GmbH, 2004

[18] Kurul N., Podowski M.Z., On the Modeling of multi-dimensional Effects in Boiling Channels, *Proc. 27th National Heat Transfer Conf*., Minneapolis, 1991

[19] Del Valle V.H., Kenning D.B.R., Subcooled Flow Boiling at High Heat Flux, *Int. J. Heat and Mass Transfer*, **28**, 1985, 1907–1920

[20] Lemmert M., Chawla L.M., Influence of Flow Velocity on Surface Boiling Heat Transfer Coefficient, in *Heat Transfer in Boiling*, E.Hahne and U.Grigull, Eds., Academic Press and Hemisphere, New York, NY, USA. 1977.

[21] Unal H.C., Bubble Diameter, Maximum Bubble Growth Time and Bubble Growth Rate During Subcooled Nucleate Boiling of Water upto 17.7 MW/m^2, *Int. J. Heat and Mass Transfer*, **19**, 1976, 643-649

[22] Cole R., A Photographic Study of Pool Boiling in the Region of the Critical Heat Flux, *AIChE Journal*, **6**, 1960, 533–542

[23] Tolubinski, V.I, Kostanchuk, D.M., Vapour Bubbles Growth Rate and Heat Transfer Intensity at Subcooled Water Boiling, *Proc. 4th Int. Heat Transfer Conf*., Paris, France, **5**, 1970, Paper number B-2.8

[24] Mani, P., Cardenas, R., and Narayanan, V., Submerged Jet Impingement Boiling on a Polished Silicon Surface, *ASME 2011 Pacific Rim Technical Conf. and Exhibition on Packaging and Integration of Electronic and Photonic Systems (InterPACK2011)*, Portland, USA, 2011, 81-94

[25] Wang D., Yu E., Przekwas A., A Computational Study of Two-Phase Jet Impingement Cooling of an Electronic Chip, *15th IEEE Semi-therm Symposium, IEEE*, 1999, 10-15

[26] Rohsenow W.M., A Method of Correlating Heat Transfer Data for Surface Boiling of Liquids, *Trans. of ASME*, **74**, 1952, 969-976

[27] Cardenas R., Submerged Jet Impingement Boiling Thermal Management, Ph.D. Thesis, Oregon State University, USA, 2011

[28] Basu N., Warrier G.R., Dhir V.K., Wall Heat Flux partitioning during subcooled flow boiling: Part I-Model Development, *ASME J. Heat Transfer*, **127**, 2005, 131-140

[29] Basu N., Warrier G.R., Dhir V.K., Wall heat flux partitioning during subcooled flow boiling: Part II-Model validation, *ASME J. of Heat Transfer*, **127**, 2005, 141-148

[30] Martin H., Heat and Mass Transfer between Impinging Gas Jets and Solid Surfaces, *Adv. Heat Transfer*, **13**, 1977, 1-60

[31] Lee J., Lee S.J., Stagnation Region Heat Transfer of a Turbulent Axisymmetric Jet Impingement, *Exp. Heat Transfer*, **12**, 1999, 137-156

[32] Zuckerman N., Lior N., Jet Impingement Heat Transfer: Physics, Correlations, and Numerical Modeling, *Adv. Heat Transfer*, **39**, 2006, 565-631

[33] Wolf D., Incropera F., Viskanta R., Local Jet Impingement Boiling Heat Transfer, *Int. J. Heat and Mass Transfer*, **39**, 1996, 1395-1406